Atomistic simulation of liquid-vapour coexistence: binary mixtures

Atomistic simulation of liquid–vapour coexistence: binary mixtures

E Salomons and M Mareschal†

CEREM-DTM-SRMP, CEN Saclay, 91191 Gif sur Yvette Cédex, France

Abstract. Liquid–vapour coexistence and surface tension of binary mixtures is studied by Monte Carlo simulation. Both mixtures with a difference in the size parameters and mixtures with a difference in the energy parameters of the Lennard–Jones potential are investigated. The results for the surface tension and the coexisting liquid density are compared with the predictions of one-fluid models. The van der Waals model is found to be quite accurate, except in cases of strong interfacial adsorption. An interpretation of this accuracy is given, by developing a one-fluid model based on random packing of hard spheres. It is found that the predictions of this random-packing model are close to predictions of the van der Waals one-fluid model. We also present a simulation of the argon–krypton liquid–vapour interface.

1. Introduction

Surface tension is a direct manifestation of the attractive interaction between atoms or molecules in a liquid. The statistical-mechanical problem of computing the surface tension and other liquid–vapour interfacial quantities from this interaction can be solved either by approximate theories or by computer simulation. The advantage of computer simulation is that no approximation has to be made, the disadvantage is the use of a finite system with truncated interatomic potentials. Several simulations of liquid–vapour systems have been reported in the literature, using either the Monte Carlo or the molecular-dynamics method (see [1]).

In binary mixtures, interesting effects occur due to adsorption at the liquid–vapour interface: adsorption of the more volatile component can significantly reduce the surface tension (this follows from the Gibbs adsorption equation). A mean field theory for inhomogeneous fluids has been developed [2], that reproduces this effect [3]. The theory predicts values of the surface tension of mixtures with reasonable accuracy, though they are generally slightly too low. Relatively few simulation studies of liquid–vapour coexistence in binary mixtures have been reported [2–5].

Recently we demonstrated that interfacial quantities obtained from Monte Carlo simulations are consistent with the Gibbs adsorption equation [5]. For binary mixtures it was further demonstrated that the inclusion of particle exchanges in the simulations leads to improved sampling of configurational phase space, and hence yields more accurate values for the ensemble averages than conventional Monte Carlo or

† Also: Université Libre de Bruxelles, Belgium.

9215

molecular-dynamics methods do. Here we apply this simulation technique to liquid-vapour coexistence in a series of binary Lennard–Jones mixtures, with energy and size parameters of the potential varied systematically (in [2–5] argon–krypton parameters were used). It should be noted that the system, consisting of a liquid film in equilibrium with its vapour, is too small to eliminate finite-size effects on interfacial quantities. Nevertheless, we think that it is an interesting model system for liquid-vapour coexistence in mixtures.

We will compare the results of the simulations with the predictions of several one-fluid models. A one-fluid model is in fact a generalization of the principle of corresponding states [6, 7]: a mixture is represented by a hypothetical pure system with suitably chosen potential parameters. Although the thermodynamic properties of the pure system are required as input, one-fluid models are very useful in understanding and predicting properties of mixtures. From simulations of homogeneous fluid mixtures it has been found that the van der Waals one-fluid (vdW1f) model is surprisingly accurate [6, 8]. We will give an interpretation of this accuracy by considering a simple model for a liquid: a random packing of hard spheres [9, 10]. From the values of the packing fraction of randomly packed hard-sphere mixtures we will construct a one-fluid model with an accuracy comparable with that of the vdW1f model.

This article is organized as follows. In section 2 we present the atomistic model, and the method of obtaining thermodynamic quantities from simulations. In section 3 one-fluid models are described. In section 4 we present the results of the simulations, and compare these with the predictions of one-fluid models.

2. Atomistic model and thermodynamic properties

Binary mixtures of 'a' and 'b' atoms are considered, with interatomic potentials given by $(i, j = a, b)$

$$\phi(r_{ij}) = 4\varepsilon_{ij} \left[\left(\frac{\sigma_{ij}}{r_{ij}} \right)^{12} - \left(\frac{\sigma_{ij}}{r_{ij}} \right)^{6} \right]. \tag{1}$$

All quantities in this article are dimensionless, reduced with respect to ε_{aa} and σ_{aa} (so that $\varepsilon_{aa} = 1$ and $\sigma_{aa} = 1$). The interatomic potentials are truncated at a cut-off radius of $R_c = 3$. For the a–b interaction the relationships $\sigma_{ab} = (\sigma_{aa} + \sigma_{bb})/2$ (Lorentz rule) and $\varepsilon_{ab} = \xi(\varepsilon_{aa}\varepsilon_{bb})^{1/2}$ (Berthelot rule for $\xi = 1$) are used.

We consider a liquid film in equilibrium with its vapour, consisting of atoms interacting through potentials given by equation (1). We are interested in the surface tension γ, and the partial density profiles $\rho_a(z)$ and $\rho_b(z)$, i.e. the number densities of 'a' atoms and 'b' atoms as a function of the position coordinate z perpendicular to the interface.

It is straightforward to obtain partial density profiles from an atomistic simulation. The total density $\rho_a(z) + \rho_b(z)$ at the centre of the liquid film (the orthobaric liquid density) is denoted by ρ^{liq}, and $v = 1/\rho^{liq}$ is the average atomic volume in the liquid. The excess liquid volume of a mixture, at reduced temperature $\tau = kT/\varepsilon_{aa}$, is defined as

$$v^{E}(\tau) = v(\tau) - x_a v_a(\tau) - x_b v_b(\tau) \tag{2}$$

where x_a and x_b are fractional liquid concentrations ($x_a + x_b = 1$), and $v_a(\tau) = v_{\text{pure}}(\tau)$ and $v_b(\tau) = \sigma_{bb}^3 v_{\text{pure}}(\tau/\varepsilon_{bb})$, in which $v_{\text{pure}}(\tau)$ is the coexisting liquid volume of the pure Lennard–Jones system with $R_c = 3$.

The surface tension is determined through the virial expression for a plane liquid–vapour interface of area A [1]:

$$\gamma = \frac{1}{2A} \left\langle \sum_{i<j} \left(1 - \frac{3z_{ij}^2}{r_{ij}^2}\right) r_{ij} \phi'(r_{ij}) \right\rangle \tag{3}$$

where r_{ij} is the distance between the atoms i and j, $\phi'(r_{ij})$ is the derivative of the pair potential (1), and angular brackets denote an ensemble average. In a previous article [5] we demonstrated that values of the surface tension determined through the virial expression are in agreement with values determined through the definition in terms of the free energy F, $\gamma = (\partial F/\partial A)_{N,V,T}$.

The long-range correction for the surface tension, i.e. the contribution of the tail of the interatomic potential beyond the cut-off radius, is given by

$$\gamma_c = \tfrac{3}{2}\pi \left(\frac{\rho^{\text{liq}}}{R_c}\right)^2 \Sigma_{i,j} x_i x_j \varepsilon_{ij} \sigma_{ij}^6. \tag{4}$$

This expression is obtained by using the approximation $g(r) \approx 1$ for $r > R_c$ ($g(r)$ is the radial distribution function), and neglecting the density of the vapour [11]. For the pure Lennard–Jones system the sum in equation (4) is equal to unity.

The excess surface tension of a mixture is defined as

$$\gamma^E(\tau) = \gamma(\tau) - x_a \gamma_a(\tau) - x_b \gamma_b(\tau) \tag{5}$$

where γ_a and γ_b are the surface tensions of components 'a' and 'b', respectively. We denote the surface tension of the pure system by γ_{pure}, so that $\gamma_a(\tau) = \gamma_{\text{pure}}(\tau)$ and $\gamma_b(\tau) = [\gamma_{\text{pure}}(\tau/\varepsilon_{bb}) + \Delta\gamma_c]\varepsilon_{bb}/\sigma_{bb}^2$ (here $\Delta\gamma_c = (\pi/6)(1 - \sigma_{bb}^2)\rho_{\text{pure}}^{\text{liq}\,2}(\tau/\varepsilon_{bb})$ is a small correction term to arrive at the proper cut-off radius for the b–b interaction).

3. One-fluid models

In the one-fluid models described in this section, a binary Lennard–Jones mixture is represented by a hypothetical pure system with parameters ε_x and σ_x. The principle of corresponding states gives

$$\rho_x^{\text{liq}}(\tau) = \sigma_x^{-3} \rho_{\text{pure}}^{\text{liq}}(\tau/\varepsilon_x) \tag{6}$$

and

$$\gamma_x(\tau) = [\gamma_{\text{pure}}(\tau/\varepsilon_x) + \Delta\gamma_c]\, \varepsilon_x/\sigma_x^2 \tag{7}$$

where $\Delta\gamma_c = (\pi/6)(1 - \sigma_x^2)\rho_{\text{pure}}^{\text{liq}\,2}(\tau/\varepsilon_x)$ is again a small correction term to arrive at the proper cut-off radius.

The simplest one-fluid model is the random-mixing (RM) approximation [12]:

$$\varepsilon_x = \left(\sum_{i,j} x_i x_j \varepsilon_{ij} \sigma_{ij}^6 \right)^2 \bigg/ \left(\sum_{i,j} x_i x_j \varepsilon_{ij} \sigma_{ij}^{12} \right) \tag{8a}$$

$$\sigma_x = \left[\left(\sum_{i,j} x_i x_j \varepsilon_{ij} \sigma_{ij}^{12} \right) \bigg/ \left(\sum_{i,j} x_i x_j \varepsilon_{ij} \sigma_{ij}^6 \right) \right]^{1/6} . \tag{8b}$$

This model is known to give a poor description of a binary mixture, unless all atoms are of the same size ($\sigma_{aa} = \sigma_{ab} = \sigma_{bb}$) [6]. It corresponds to the assumption that all radial distribution functions are equal: $g_{ij}(r) = g_x(r)$ for all i, j. A more realistic assumption is [7, 13]: $g_{ij}(r/\sigma_{ij}) = g_x(r/\sigma_x)$ for all i, j. Substitution in the energy equation (relating the interaction energy to the radial distribution functions) gives [7]

$$\varepsilon_x \sigma_x^3 = \sum_{i,j} x_i x_j \varepsilon_{ij} \sigma_{ij}^3 \tag{9a}$$

and substitution in the compressibility equation (relating fluctuations in the number density to the radial distribution functions) gives [14]

$$\sigma_x^3 = \sum_{i,j} x_i x_j \sigma_{ij}^3 . \tag{9b}$$

Equations (9a) and (9b) represent the vdW1f approximation [14, 15]. Comparison with computer simulations of homogeneous mixtures has shown, that the accuracy of the vdW1f approximation is comparable with the accuracy of hard-sphere perturbation theories [6, 8].

In the following we develop a third one-fluid model, which we call a random-packing (RP) model, as it makes use of the concept of random packing of hard spheres. Values of thermodynamic quantities computed with this model turn out to be very close to values computed with the vdW1f model. One of the reasons to develop the RP model, is to gain some insight into the accuracy of the vdW1f model.

A simple model for a liquid (or dense fluid) is a random packing of hard spheres. This was realized thirty years ago, from the observation that the radial distribution function $g(r)$ of a random close packing of hard spheres is remarkably similar to the $g(r)$ of liquid argon [9, 10]. Later, it was demonstrated theoretically that the structure of a liquid is determined primarily by short-range repulsive forces [16, 7].

The packing fraction p of a system of hard spheres is the fraction of volume that is occupied by material. Application of this definition to a binary mixture of spheres with diameters $\sigma_{aa} = 1$ and $\sigma_{bb} \neq 1$, gives

$$p(\sigma_{bb}) = \rho(\sigma_{bb}) \frac{\pi}{6} \sum_{i=a,b} x_i \sigma_{ii}^3 \tag{10}$$

where x_a and x_b are the fractional concentrations of 'a' and 'b' spheres, respectively, and the dependence of p and ρ on σ_{bb} has been indicated explicitly. Hence

$$\frac{\rho(\sigma_{bb})}{\rho(\sigma_{bb} = 1)} = \frac{1}{\sum_i x_i \sigma_{ii}^3} \frac{p(\sigma_{bb})}{p(\sigma_{bb} = 1)} . \tag{11}$$

This leads us to the following expression for the parameter σ_x of the RP model

$$\sigma_x^3 = \sum_i x_i \sigma_{ii}^3 \frac{p(\sigma_{bb} = 1)}{p(\sigma_{bb})}. \tag{12}$$

We show below, that for $0.8 \leqslant \sigma_{bb} \leqslant 1.25$ the packing fraction is approximately constant, the variation being 1.6% at most. This means that the factor $p(\sigma_{bb} = 1)/p(\sigma_{bb})$ in equation (12) can be set equal to unity, in a good approximation.

In the case of a mixture with only size effects, i.e. $\varepsilon_{aa} = \varepsilon_{ab} = \varepsilon_{bb} = 1$, equation (12) is sufficient to define the RP model (setting $\varepsilon_x = 1$). This is the case considered in section 4.4. In section 4.3, we consider the case of a mixture with only energy effects, i.e. $\sigma_{aa} = \sigma_{ab} = \sigma_{bb} = 1$. In this case, the RM and the vdW1f model yield the same expression for ε_x

$$\varepsilon_x = \sum_{i,j} x_i x_j \varepsilon_{ij} \tag{13}$$

i.e. ε_x is simply a weighted average of the different ε parameters. In section 4.5 we consider the argon–krypton system, with $\varepsilon_{aa} \neq \varepsilon_{bb}$ and $\sigma_{aa} \neq \sigma_{bb}$. If one wants to use the RP model in this case, an additional equation is required to fix the parameter ε_x. We will use equation (9a), as it is based on a realistic assumption for the radial distribution functions.

In the following we give a justification of the approximation $p(\sigma_{bb} = 1)/p(\sigma_{bb}) \approx 1$ in equation (12).

Random packing of hard spheres is studied conveniently by computer construction. Several algorithms can be used to construct a random packing in a computer, just as there are several methods of preparing a random packing in reality (shaking etc). We used an algorithm similar to that described by Bennett [17]. Details of these computations will be published elsewhere [18], here we only present the results. For identical spheres (i.e. a mixture with $\sigma_{bb} = 1$) we obtained a packing fraction of $p = 0.6055$, in agreement with the value found by Bennett [17] ($p = 0.61$). For an equimolar mixture of spheres with diameters $\sigma_{aa} = 1$ and $\sigma_{bb} = 0.8$ we obtained $p = 0.6155$, i.e. only 1.6% higher than the value for $\sigma_{bb} = 1$. These results are consistent with the results of Visscher and Bolsterli [19], who also studied random packing of hard-sphere mixtures by computer construction.

It is interesting to note, that the RP model yields a zero excess liquid volume if the approximation $p(\sigma_{bb} = 1)/p(\sigma_{bb}) \approx 1$ is used. This follows directly from equations (12) and (2). Almost thirty years ago, Alder [20] found by molecular-dynamics simulations that the excess volume of hard-sphere mixtures is nearly zero. The same is true for Lennard–Jones mixtures with only size differences [6]. In section 4.4 this point is discussed further.

4. Simulations

In this section results of Monte Carlo simulations are presented, and compared with predictions of one-fluid models.

4.1. Simulation method

Simulations are performed on equimolar binary mixtures of $N = 256$ atoms ($N_a = N_b = \frac{1}{2}N$), with interatomic potentials given by equation (1). A liquid film is prepared in a rectangular simulation box with sides of length L_x, L_y and L_z (typically, $L_x = L_y = 7$ and $L_z = 14$), using periodic boundary conditions in the x-, y- and z-directions. The film is oriented perpendicular to the z-axis.

For efficient sampling of configurational phase space, we used the following variant of the Monte Carlo method [5, 21]. In addition to conventional displacements of atoms, exchanges of dissimilar atoms are also allowed. Both displacements and exchanges are accepted or rejected according to the Metropolis transition probability, i.e. satisfying detailed balance. A simulation consists of 3×10^5 displacement attempts per atom (including 0.5×10^5 attempts per atom for equilibration), and $\frac{1}{2}N$ exchange attempts are performed after each 10 (sections 4.4 and 4.5) or 25 (section 4.3) displacement attempts per atom. The liquid density (the density at the centre of the liquid film) is determined from a smooth curve through the density profile. The surface tension is determined using the virial expression (3). From a standard statistical analysis (for details, see [5]) we determined an uncertainty of ± 0.02 in the value of the surface tension (± 0.04 in the excess surface tension). The uncertainty in the coexisting liquid density is estimated at ± 0.005 (± 0.01 in the excess liquid volume). The centre of mass is kept fixed in a simulation, since otherwise a spurious broadening of the liquid–vapour interface would occur, owing to random movements of the centre of mass [5].

4.2. Pure system

Simulations of the pure Lennard–Jones system were performed at seven different temperatures τ, with $0.68 < \tau \leqslant 1.0$. Values of the surface tension and the coexisting liquid density are presented in table 1. Figure 1 shows a plot of the surface tension as a function of temperature. The straight line in this figure is a fit, given by $\gamma_{\text{pure}}(\tau) = 1.917 - 1.646\tau$. Taking into account the long-range correction, this fit is in close agreement with the fit of Rowlinson and Widom [1] to previous results of simulations of the Lennard–Jones system. The liquid density is represented by the fit $\rho_{\text{pure}}^{\text{liq}}(\tau) = 0.9002 + 0.186\tau - 0.4203\tau^2$.
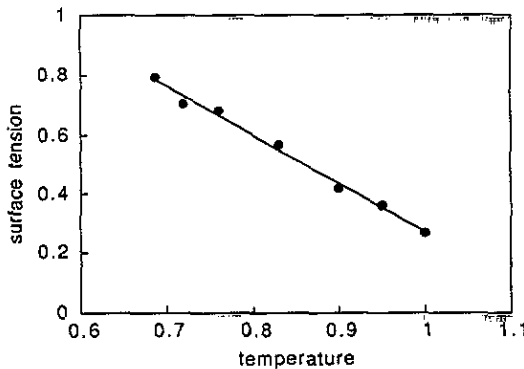

Figure 1. Surface tension of Lennard–Jones liquid–vapour system with cut-off radius $R_c = 3$

Table 1. Simulation results for the pure Lennard–Jones system, using a simulation box with $L_x = L_y = 6.72$ and $L_z = 13.44$ (section 4.2).

τ	γ	ρ_{liq}
0.6867	0.79	0.830
0.72	0.70	0.815
0.76	0.68	0.800
0.83	0.57	0.765
0.90	0.42	0.725
0.95	0.36	0.700
1.00	0.27	0.665

4.3. Mixtures of atoms of equal size

Simulations were performed on equimolar mixtures of atoms of equal size, i.e., with $\sigma_{aa} = \sigma_{ab} = \sigma_{bb} = 1$. For all mixtures we used $\varepsilon_{bb} = 1.31$ (the same value as used in [4, 5] to model the argon–krypton system with atoms of equal size), while we varied the parameter ε_{ab}, or equivalently the Berthelot parameter ξ.
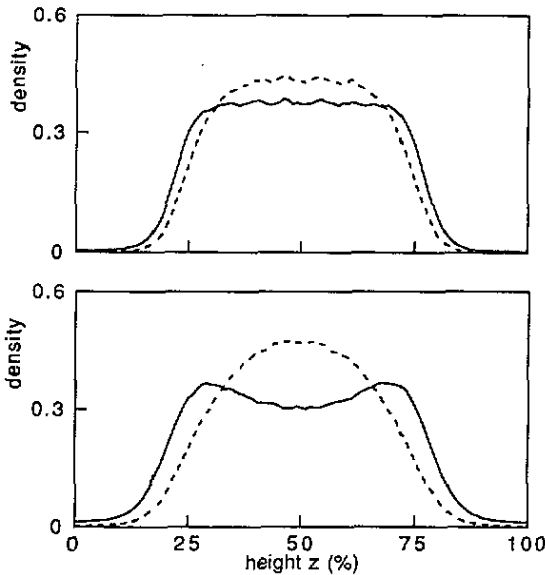

Figure 2. Density profiles for temperature $\tau = 0.9$, $\xi = 1.145$ (top) and $\xi = 0.874$ (bottom): full curves, a atoms; broken curves, b atoms.

Figure 2 shows two density profiles at temperature $\tau = 0.9$, one for Berthelot parameter $\xi = 1.145$, and one for $\xi = 0.874$. These profiles demonstrate the general trend observed in the simulations described in this section. For $\xi = 0.874$ a strong adsorption of component 'a' occurs, leading to a maximum in $\rho_a(z)$ near the interface. With increasing ξ, this maximum decreases gradually, and has disappeared completely at $\xi = 1.145$.

In figure 3 values of the orthobaric liquid density, and the corresponding values of the excess liquid volume, are plotted as a function of Berthelot parameter ξ, for three different temperatures. In figure 4 values of the surface tension, and corresponding values of the excess surface tension, are plotted as a function of ξ. All results are also
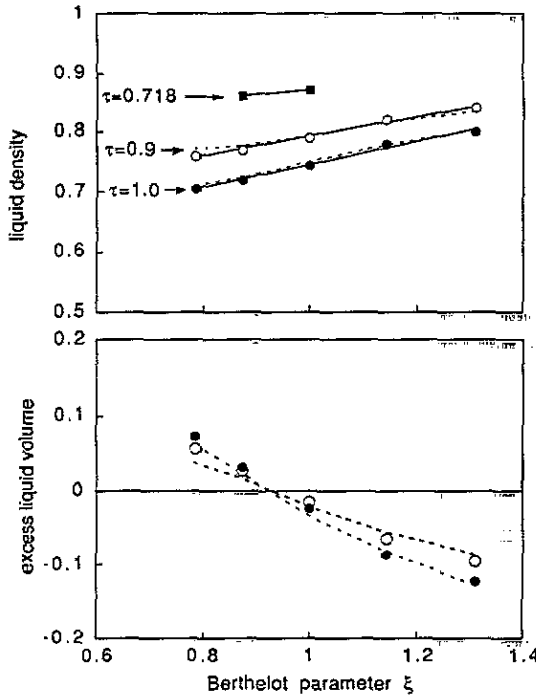
Figure 3. Liquid density and excess liquid volume of equi-sized Lennard–Jones mixtures as a function of ξ: broken curves, one-fluid models (in excess plot, thick curve $\tau = 0.9$; thin curve $\tau = 1.0$); full lines, guide to the eye; squares, $\tau = 0.718$; open circles, $\tau = 0.9$; filled circles, $\tau = 1.0$.

represented in table 2 (here x_a is the liquid concentration of component 'a'). Full lines in figures 3 and 4 are guides to the eye, while broken curves represent one-fluid models, which are all identical in this case (see equation (13)). For temperature $\tau = 0.718$ we have no prediction of one-fluid models, as this temperature is too low to apply equations (6) and (7) (the temperature of the hypothetical pure system falls outside the range of validity of the fits for the pure Lennard–Jones system, i.e. below the triple-point temperature).

For the liquid density and the excess volume, the predictions of one-fluid models are in close agreement with simulation results (figure 3). For the surface tension (figure 4) the agreement is good for $\xi \gtrsim 1$, while for $\xi < 1$ the simulation results are systematically lower than the predictions of one-fluid models. This systematic deviation is a consequence of the effect mentioned in the introduction of this article: interfacial adsorption of the more volatile component in a binary mixture causes a reduction of the surface tension. Indeed, density profiles show strong interfacial adsorption for $\xi < 1$ (see figure 2). The explanation of this effect is obvious: the surface tension is most sensitive to the composition near the interface, so that interfacial adsorption of the more volatile component, which has a weaker interatomic attraction than the other component, reduces the surface energy and hence the surface tension (with respect to the value expected from the bulk liquid composition). From a thermodynamic point of view, the effect follows from the Gibbs adsorption equation.
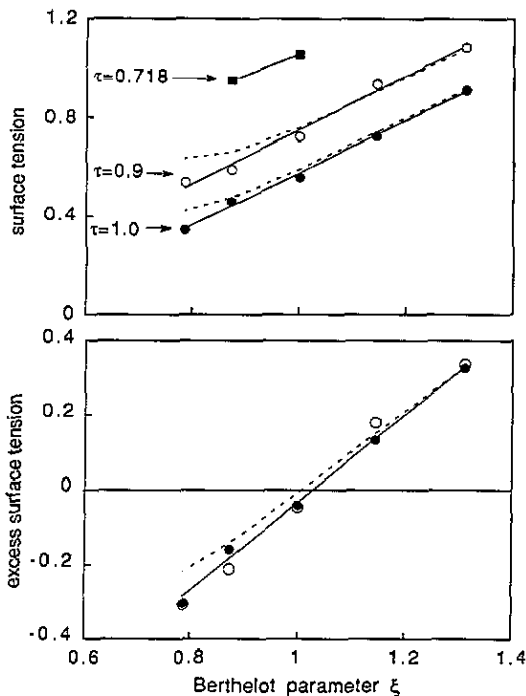
Figure 4. Surface tension and excess surface tension of equi-sized Lennard–Jones mixtures as a function of ξ. Broken curves: one-fluid models; full lines: guide to the eye. Squares, $\tau = 0.718$; open circles, $\tau = 0.9$; filled circles, $\tau = 1.0$.

Table 2. Simulation results for equimolar mixtures with $\sigma_{aa} = \sigma_{ab} = \sigma_{bb} = 1$ and $\varepsilon_{bb} = 1.31$, using a simulation box with $L_x = L_y = 6.72$ and $L_z = 13.44$ (section 4.3).

τ	ξ	γ	ρ^{liq}	x_a
0.718	1	1.06	0.870	0.425
0.718	0.874	0.95	0.860	0.314
0.9	1.310	1.09	0.840	0.476
0.9	1.145	0.93	0.820	0.463
0.9	1	0.72	0.790	0.443
0.9	0.874	0.59	0.770	0.390
0.9	0.786	0.54	0.760	0.316
1.0	1.310	0.91	0.800	0.475
1.0	1.145	0.72	0.780	0.462
1.0	1	0.56	0.745	0.450
1.0	0.874	0.46	0.720	0.417
1.0	0.786	0.34	0.705	0.369

4.4. Mixtures of atoms of different size

Simulations were performed on equimolar mixtures with $\varepsilon_{aa} = \varepsilon_{ab} = \varepsilon_{bb} = 1$ and $0.8 \leqslant \sigma_{bb} \leqslant 1.2$. Figure 5 shows the density profile obtained for a mixture with $\sigma_{bb} = 1.2$, at temperature $\tau = 0.718$.

In figure 6 values of the coexisting liquid density, and corresponding values of the excess liquid volume, are represented by filled symbols, as a function of the parameter
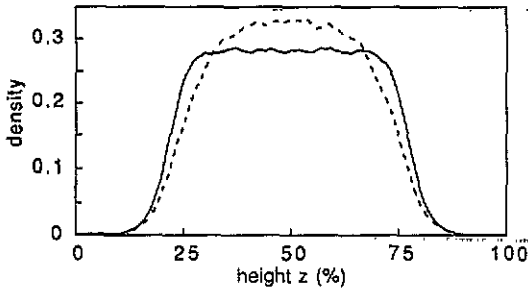
Figure 5. Density profile for $\tau = 0.718$ and $\sigma_{bb} = 1.2$: broken curve, a atoms; full curve, b atoms.
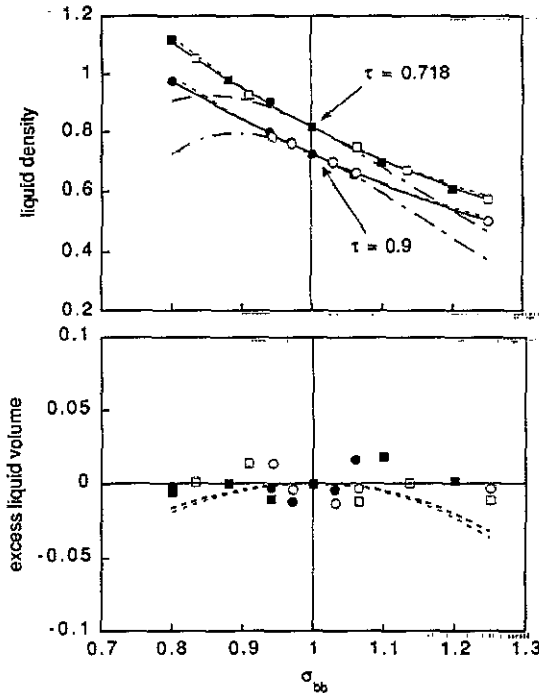

Figure 6. Coexisting liquid density and excess liquid volume as a function of σ_{bb}: long–short broken curves, RM; full curves, RP; broken curves, vdW1f. In the excess plot, thick curve ($\tau = 0.718$), thin curve ($\tau = 0.9$).

σ_{bb}. In figure 7 values of the surface tension, and corresponding values of the excess surface tension, are represented by filled symbols. All results are also represented in table 3.

Symmetry with respect to $\sigma_{bb} = 1$ leads to the relations:

$$\rho^{liq}(1/\sigma_{bb}) = \sigma_{bb}^3 \rho^{liq}(\sigma_{bb}) \tag{14}$$

$$\gamma(1/\sigma_{bb}) = \sigma_{bb}^2 \left[\gamma(\sigma_{bb}) + \Delta\gamma_c\right] \tag{15}$$

with $\Delta\gamma_c = (\pi/6)(1 - \sigma_{bb}^{-2})\rho_{pure}^{liq\ 2}$. Open symbols in figures 6 and 7 represent values calculated with these relations. They are in good agreement with direct simulation values.

Table 3. Simulation results for equimolar mixtures with $\varepsilon_{aa} = \varepsilon_{ab} = \varepsilon_{bb} = 1$, using a simulation box with $L_x = L_y = \frac{1}{2}L_z = 7.39$ for $\sigma_{bb} = 1.2, L_x = L_y = \frac{1}{2}L_z = 7.06$ for $\sigma_{bb} = 1.1$, and $L_x = L_y = \frac{1}{2}L_z = 6.72$ otherwise (section 4.4).

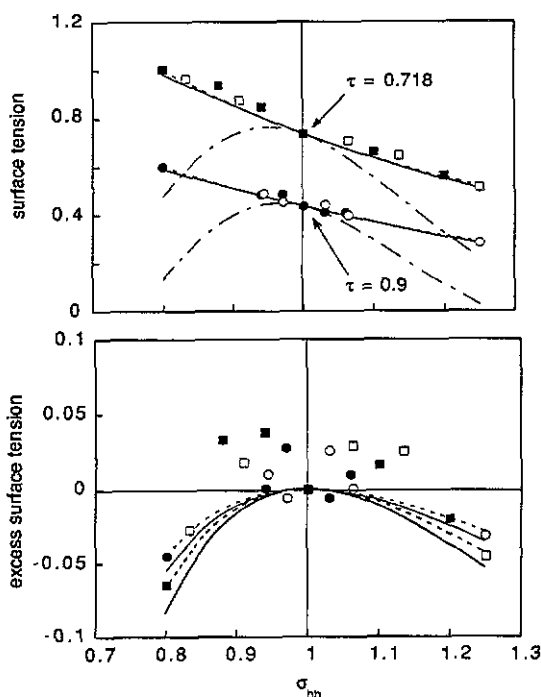| τ	σ_{bb}	γ	ρ^{liq}	x_a
0.718	0.8	1.01	1.120	0.451
0.718	0.88	0.94	0.980	0.469
0.718	0.94	0.85	0.900	0.489
0.718	1.1	0.66	0.695	0.525
0.718	1.2	0.56	0.610	0.541
0.9	0.8	0.60	0.975	0.477
0.9	0.94	0.48	0.795	0.491
0.9	0.97	0.49	0.765	0.497
0.9	1.03	0.41	0.695	0.504
0.9	1.06	0.41	0.655	0.504

Figure 7. Surface tension and excess surface tension as a function of σ_{bb}. Long–short broken curves, RM; full curves, RP; broken curves, vdW1f. In the excess plot, thick curves ($\tau = 0.718$), thin curves ($\tau = 0.9$).

One-fluid models are represented by the different curves in figures 6 and 7. The RM approximation fails even for small deviations from the value $\sigma_{bb} = 1$. The vdW1f model and the RP model [using $p(\sigma_{bb}) =$ constant] work much better. The agreement is excellent for the liquid density and the excess volume (figure 6). For the surface tension (figure 7) the agreement is reasonable. The numerical difference between the vdW1f model and the RP model is small.

Simulation values of the excess liquid volume v^E are nearly zero over the full range

$0.8 \leqslant \sigma_{bb} \leqslant 1.25$ (figure 6). The vdW1f model yields slightly negative values for v^E. The RP model yields a zero excess liquid volume if the approximation $p(\sigma_{bb} = 1)/p(\sigma_{bb}) \approx 1$ is used (see section 3). If instead the values $p(\sigma_{bb} = 1) = 0.6055$ and $p(\sigma_{bb} = 0.8) = 0.6155$ are used (see section 3), the RP model yields $v^E = -0.015$ for $\sigma_{bb} = 0.8$, and $v^E = -0.03$ for $\sigma_{bb} = 1.25$ [using $p(1/\sigma_{bb}) = p(\sigma_{bb})$]. These values are very close to the values predicted by the vdW1f model (see figure 6).

4.5. Argon–krypton system

We performed a simulation of an equimolar mixture with Lennard–Jones parameters appropriate to the argon–krypton system [8]: $\varepsilon_{bb} = 1.394$, $\xi = 0.989$, $\sigma_{bb} = 1.067$. A temperature of $\tau = 0.948$ was used. The density profile (figure 8) shows a substantial adsorption of argon at the interface. The results we obtained for the surface tension and the coexisting liquid density are represented in table 4, together with predictions of one-fluid models.
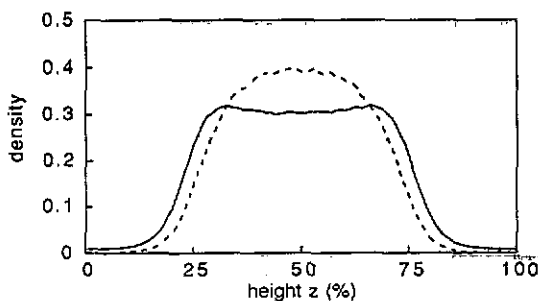

Figure 8. Density profile for argon–krypton system at $\tau = 0.948$: full curve, argon; broken curve, krypton.

Table 4. Simulation results for equimolar argon–krypton mixture, using a simulation box with $L_x = L_y = 7.15$ and $L_z = 14.30$ (section 4.5).

	γ	ρ^{liq}
MC	0.67	0.700
RM	0.624	0.685
RP	0.684	0.704
vdW1f	0.688	0.706

The simulation results lead to an excess surface tension of $\gamma^E = 0.00$ (inclusion of the long-range correction does not change this value) and an excess liquid volume of $v^E = -0.019$. The value of the excess volume is in good agreement with the experimental value for the argon–krypton system [13]: $v^E = -0.022$. The value of the excess surface tension deviates from the experimental value [22] $\gamma^E = -0.056$, but this deviation is only slightly larger than the statistical error bar of ± 0.04.

5. Conclusions

A systematic study has been presented of liquid–vapour coexistence in binary Lennard–Jones mixtures. The effect of the energy parameter and the effect of the

size parameter have been investigated separately. In mixtures of atoms of equal size, strong interfacial adsorption of the more volatile component occurs for Berthelot parameter $\xi < 1$. This adsorption causes a significant reduction of the surface tension (with respect to the value expected from the bulk liquid composition). The size effect has been studied by simulations of mixtures with equal energy parameters. It has been found that in the range $0.8 \leqslant \sigma_{bb} \leqslant 1.25$ both the excess surface tension and the excess liquid volume are small.

Two general points emerge from this work:

(i) accurate values of liquid–vapour interfacial properties of mixtures can be obtained from atomistic simulations; and

(ii) one-fluid approximations (vdW1f and RP) can be used to predict these values.

As for the first point, it is essential to include exchanges of dissimilar atoms in the simulations, to avoid ergodicity problems. This leads to density profiles with relatively small spatial fluctuations, and values of the surface tension with a statistical accuracy of ± 0.02. In the future, with the increasing power of computers, it is desirable to go to larger systems, to exclude finite-size effects on interfacial properties.

As for the second point, it has been shown that the vdW1f model is very accurate in predicting the coexisting liquid density, and reasonably accurate in predicting the surface tension. The effect of interfacial adsorption on the surface tension, however, is not taken into account by one-fluid models (although an attempt has been made to take adsorption into account in the RM approximation [12]).

We have given an interesting interpretation of the accuracy of the vdW1f model, by developing the conceptually simple RP model, which yields values that differ numerically very little from vdW1f values. Whereas the vdW1f model (equation $(9b)$) follows from consideration of density *fluctuations*, the RP model (equation (12)) is obtained from consideration of the density itself. Application of the RP model requires values of the packing fraction of hard-sphere mixtures, which can be calculated by computer construction. This implies that application of the RP model is not as straightforward as application of the vdW1f model (except in the range $0.8 \lesssim \sigma_{bb} \lesssim 1.25$, where the packing fraction is constant, in good approximation). On the other hand, the range of validity (in terms of the size ratio σ_{bb}/σ_{aa}) is expected to be larger for the RP model than for the vdW1f model. Even in the extreme case where the size ratio is so small (or large) that the small spheres fit entirely in the voids between the close-packed large spheres (we use the hard-sphere picture of a liquid here), the RP model might still be a reasonable approximation.

Acknowledgments

References

[1] Rowlinson J S and Widom B 1982 *Molecular Theory of Capillarity* (Oxford: Clarendon)
[2] Lee D J, Telo da Gama M M and Gubbins K E 1984 *Mol. Phys.* **53** 1113
[3] Lee D J, Telo da Gama M M and Gubbins K E 1985 *J. Phys. Chem.* **89** 1514

[4]   Chapela G A, Saville G, Thompson S M and Rowlinson J S 1977 *J. Chem. Soc., Faraday Trans.*
      II **73** 1133
[5]   Salomons E and Mareschal M 1991 *J. Phys.: Condens. Matter* **3** 3645
[6]   Rowlinson J S and Swinton F L 1982 *Liquids and Liquid Mixtures* (London: Butterworths)
[7]   Hansen J P and McDonald I R 1986 *Theory of Simple Liquids* (London: Academic)
[8]   McDonald I R 1972 *Mol. Phys.* **23** 41
[9]   Bernal J D 1959 *Nature* **183** 141
      Bernal J D and King S V 1968 *Physics of Simple Liquids* ed H N V Temperley, J S Rowlinson
      and G S Rushbrooke (Amsterdam: North-Holland)
[10] Scott G D 1962 *Nature* **194** 956
[11] Fowler R H 1937 *Proc. R. Soc.* A **159** 229
[12] Defay R, Prigogine I, Bellemans A and Everett D H 1966 *Surface Tension and Adsorption*
      (London: Longmans)
[13] Henderson D and Leonard P J 1971 *Physical Chemistry – An Advanced Treatise* vol 8B, ed
      H Eyring, D Henderson and W Jost (New York: Academic) ch 7
[14] MacGowan D, Lebowitz J L and Waisman E M 1985 *Chem. Phys. Lett.* **114** 321
[15] Leland T W, Rowlinson J S and Sather G A 1968 *Trans. Faraday Soc.* **64** 1447
[16] Weeks J D, Chandler D and Andersen H C 1971 *J. Chem. Phys.* **54** 5237
[17] Bennett C H 1972 *J. Appl. Phys.* **43** 2727
[18] Salomons E and Mareschal M 1991 *Europhys. Lett.* **16** 85
[19] Visscher W M and Bolsterli M 1972 *Nature* **239** 504
[20] Alder B J 1964 *J. Chem. Phys.* **40** 2724
[21] Kranendonk W G T and Frenkel D 1989 *J. Phys.: Condens. Matter* **1** 7735
[22] Nadler K C, Zollweg J A, Streett W B and McLure I A 1988 *J. Colloid Interface Sci.* **122** 530